A Finite Element Model for Bone Ingrowth into a Prosthesis

F.J. Vermolen, E.M. van Aken, J.C. van der Linden, and A. Andreykiv

Abstract We consider a finite element method for a model of bone ingrowth into a prosthesis. Such a model can be used as a tool for a surgeon to investigate the bone ingrowth kinetics when positioning a prosthesis. The overall model consists of two coupled models: the biological part that consists of non-linear diffusion-reaction equations for the various cell densities and the mechanical part that contains the equations for poro-elasticity. The two models are coupled and in this paper the model is presented with some preliminary academic results. The model is used to carry out a parameter sensitivity analysis of ingrowth kinetics with respect to the parameters involved.

1 Introduction

In osteoporosis, fracture risk is high, after a hip fracture a joint that replaces the prosthesis is often the only remedy. In the case of osteoarthritis and rheumatoid arthritis, the cartilage degrades and moving the joints becomes painfull. Ultimately, most patients will receive a prosthesis to restore the function of a diseased joint. Prostheses, which are fixed in the bone by bone ingrowth in a porous layer are usually put in the bone using a screw, to obtain sufficient initial stability. Bone will grow into a porous tantalum layer in the course of time, and hence more stability of the prosthesis is obtained. To investigate the quality and life time of such an artificial joint, one needs to study the effects of the placement of the prosthesis and of the

F.J. Vermolen and E.M. van Aken
Delft Institute of Applied Mathematics, Faculty of Electrical Engineering, Mathematics and Computer Science, Delft University of Technology, Mekelweg 4, 2628 CD Delft, The Netherlands
e-mail: F.J.Vermolen@tudelft.nl,

J.C. van der Linden and A. Andreykiv
Mechanical, Maritime and Materials Engineering, Delft University of Technology, Mekelweg 2, 2628 CD Delft, The Netherlands

materials that are involved in the joint. At present, these effects are often studied using large amounts of data of patients. To predict the life span and performance of artificial joints, numerical simulations are necessary since these simulations give many qualitative insights by means of parameter sensitivity analysis. These insights are hard to obtain by experiments.

Several studies have been done to simulate bone-ingrowth or fracture healing of bones. To list a few of them, we mention the model due to Adam [1], Ament and Hofer [3], Bailon-Plaza *et al.* [5], Huiskes *et al.* [9] and recently by Andreykiv [4]. The model due to Huiskes *et al.* and LaCroix *et al.* [9, 11] will be treated in more detail, since we expect that this model contains most of the biologically relevant processes, such as cell division and differentiation, tissue regeneration, and cell mobilility. Many ideas from modeling fracture healing of bones are used in these models, since bone-ingrowth into a prosthesis resembles the fracture healing process. In the model due to Huiskes, the influence of the mechanical properties on the biological processes are incorporated. Further, we note that Huiskes' model has been compared to animal experiments.

In this paper, we will see a calibrated existing bone ingrowth model (and its numerical solution) in terms of a system of nonlinearly coupled equations from diffusion, reactions and poro-elasticity. This paper concerns a compilation of preliminary results, with some data for a shoulder prosthesis.

2 The Model

Huiskes [9] considers the behavior of mesenchymal cells, that originate from the bone marrow and differentiate into fibroblasts, chondrocytes and osteoblasts. These newly created cell types respectively generate fibrous tissue, cartilage and bone. In Huiskes' model, it is assumed that fibroblasts may differentiate into chondrocytes, chondrocytes may differentiate into osteoblasts. The differentiation processes are assumed to be nonreversible. The differentiation pattern has been sketched in Figure 1. The accumulation at a certain location of all the cell types is determined by

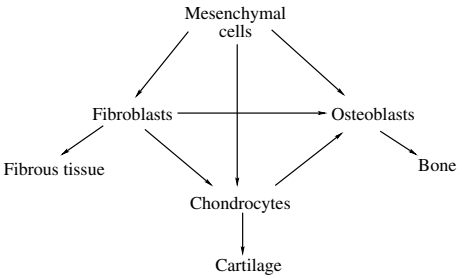

Fig. 1 The scheme of cell differentiation of mesenchymal cells, fibroblasts, chondrocytes and osteoblasts.

cell mobility, cell division and cell differentiation. Let c_m, c_c, c_f and c_b respectively denote the cell density of the mesenchymal cells, chondrocytes, fibroblasts and osteoblasts, in the poro-elastic tantalum of the prosthesis in which bone ingrowth takes place, then, the dynamics of the cell densities are described by

$$\begin{aligned}\frac{\partial c_m}{\partial t} &= \operatorname{div} D_m \operatorname{grad} c_m + P_m(1-c_{\text{tot}})c_m + \\ &\quad -F_f(1-c_f)c_m - F_c(1-c_c)c_m - F_b(1-c_b)c_m, \\ \frac{\partial c_f}{\partial t} &= \operatorname{div} D_f \operatorname{grad} c_f + P_f(1-c_{\text{tot}})c_f + \\ &\quad -F_f(1-c_f)c_m - F_c(1-c_c)c_f - F_b(1-c_b)c_f,\end{aligned} \tag{1}$$

where the diffusivities, D_m and D_f, of the mobile cells are determined by the volume fractions of tissues, being denoted by m_c and m_b for cartilage and bone respectively, by

$$\begin{aligned}D_i &= D_i^0(1-m_c-m_b), \\ P_i &= P_i^0(1-m_c-m_b),\end{aligned} \qquad i \in \{m,f\}. \tag{2}$$

The chondrocytes and osteoblasts, respectively producing cartilage and bone, are assumed to be immobile. Their reaction processes are modeled by

$$\begin{aligned}\frac{\partial c_c}{\partial t} &= P_c(1-c_{\text{tot}})c_c + F_c(1-c_c)(c_m+c_f) - F_b(1-c_b)c_c, \\ \frac{\partial c_b}{\partial t} &= P_b(1-c_{\text{tot}})c_b + F_b(1-c_b)(c_m+c_f+c_c).\end{aligned} \tag{3}$$

The tissues, fibrous tissue, cartilage and bone are immobile. Let the volume fraction of fibrous tissue be denoted by m_f, then the accumulation of these tissues is modeled by

$$\begin{aligned}\frac{\partial m_f}{\partial t} &= Q_f(1-m_{\text{tot}})c_f - (D_b c_b + D_c c_c)m_f m_{\text{tot}}, \\ \frac{\partial m_c}{\partial t} &= Q_c(1-m_b-m_c)c_c - D_b c_b m_c m_{\text{tot}}, \\ \frac{\partial m_b}{\partial t} &= Q_b(1-m_b)c_b.\end{aligned} \tag{4}$$

The initial concentrations of all tissues and cell types are zero. As boundary conditions, a Dirichlet condition for the mesemchymal cell density at the bone implant and homogeneous Neumann conditions at all other boundaries are applied. In the present paper, the influence of the micromotions is neglected. For the fibroblasts homogeneous Neumann boundary conditions are imposed for all boundary segments. The proliferation, differentiation and diffusion parameters depend on the mechanical stimulus. The mechanical stimulus is given by a linear combination of the maximum shear strain and the fluid velocity relative to the rate of displacement of the solid, that is

$$S = \frac{\gamma}{a} + \frac{v}{\beta}, \tag{5}$$

where γ represents the maximum shear strain and v denotes the relative fluid/solid velocity. Here $\gamma := \frac{1}{2}(\lambda_1 - \lambda_2)$, where $\lambda_{1,2}$ represent the eigenvalues of the strain tensor. The rates of tissue regeneration and differentiation qualitatively depends on the mechanical parameters such that:

- Low strain has a stimulatory effect (in relation to no strain) on the fibroblast proliferation and bone regeneration (if $0 < S < 1$);
- For intermediate values of the strain, cartilage formation is more favorable (if $1 < S < 3$);
- High strains favor the proliferation of fibrous tissue (if $S > 3$).

This gives a coupling of the poro-elasticity model to this biological model. The above set of partial differential equations poses a nonlinearly coupled set of equations. Standard Galerkin Finite Element methods provide a straightforward method to obtain solutions. To get the local strains and stresses in the porous tantalum that are required for the differentiation and mobility characteristics, the equations for poro-elasticity are solved. The model was derived by Biot originally. We will give an explanation for two-dimensional domains. In the poro-elastic domain where $\mathbf{u} = [u\ v]^T$ denote the displacement in the x- and $y-$ direction, we have:

$$\begin{aligned} &-\text{div}\ (\mu\ \text{grad}\ u) - \frac{\partial}{\partial x}((\lambda+\mu)\ \text{div}\ \mathbf{u}) + \frac{\partial p}{\partial x} = 0, \\ &-\text{div}\ (\mu\ \text{grad}\ v) - \frac{\partial}{\partial y}((\lambda+\mu)\ \text{div}\ \mathbf{u}) + \frac{\partial p}{\partial y} = 0, \\ &\frac{\partial}{\partial t}(n_f \beta_f p + \text{div}\ \mathbf{u}) - \text{div}\ \left(\frac{\kappa}{\eta}\ \text{grad}\ p\right) = 0. \end{aligned} \tag{6}$$

Here κ denotes the permeability, η the viscosity, n_f the porosity and finally β_f represents the compressibility. Furthermore, μ and λ are the Lamé parameters that originate from the stiffness and Poisson's ratio of the material. These parameters have to be updated as bone grows into the prosthesis. The Rule of Mixtures is applied to update the mechanical properties (see Lacroix & Prendergast [11]). For more information on the derivation of the above equations, we refer to Bear [6].

Next, we consider a scaled version of equations (6), in which we draw our attention to the third equation. In this scaling argument, we assume that the coefficients in the equations (6) are constant in time and space. Division of this equation by $n_f \beta_f$ (under the assumption that n_f and β_f are constant), and using the dimensionless variables $X, Y := \frac{x,y}{L}$, $\tau := \frac{\kappa}{\eta \beta_f n_f}\frac{t}{L^2}$, and $U, V := \frac{u,v}{L}$, where L is a characteristic length. Then equations (6) change into

$$\begin{aligned} &-\overline{\nabla}\cdot(\mu\ \overline{\nabla}\ U) - \frac{\partial}{\partial X}((\lambda+\mu)\ \overline{\nabla}\ \cdot \mathbf{U}) + \frac{\partial p}{\partial X} = 0, \\ &-\overline{\nabla}\cdot(\mu\ \overline{\nabla}\ V) - \frac{\partial}{\partial Y}((\lambda+\mu)\ \overline{\nabla}\ \cdot \mathbf{U}) + \frac{\partial p}{\partial Y} = 0, \\ &\frac{\partial}{\partial \tau}(\overline{\nabla}\cdot\ \mathbf{U}) = n_f \beta_f \left(\overline{\Delta} p - \frac{\partial p}{\partial \tau}\right). \end{aligned} \tag{7}$$

where $\overline{\nabla}(.) := \frac{1}{L}\nabla(.)$, $\overline{\Delta}(.) := \frac{1}{L^2}\Delta(.)$ and $\mathbf{U} := \frac{1}{L}\mathbf{u}$. We see that as $n_f\beta_f \to 0$, then, we reach the incompressible limit, which gives a saddle-point problem where one has to consider LBB condition satisfying elements or a stabilization. The situation becomes analogous to the Stokes' equations.

3 The Method

For a rather recent comprehensive overview of Finite Element methods applied to solid state mechanics, we refer to the book due to Bræss [7]. The above poro-elasticity equations are often solved using non-conforming Finite element methods, such as the Taylor-Hood family: if the pressure is approximated with elements of polynomials of P_n, then, the displacements are approximated using polynomials of P_{n+1}. In the Taylor-Hood elements, one usually uses linear and quadratic basis functions for the pressure and displacements respectively. On the other hand, Crouzeix-Raviart elements, which are often used for Stokes flow problems, are based on a discontuity of the pressure. Since $p \in H^1(\Omega) \subset C(\Omega)$, the Crouzeix-Raviart elements are not suitable here. As long as the compressibility is sufficiently large, one can also make use of linear-linear elements for the pressure and displacement. This was done successfully in the study due to Andreykiv [4]. If $\beta_f = 0$, which is the incompressible case, then the issue of oscillations and the use of appropriate elements or a stabilization becomes more important. For $\beta_f = 0$, the third equation in equation (6) reduces to the version that is solved by Aguilar *et al.* [2].

A Galerkin formulation of the above equation with

$$p = \sum_{j=1}^{m} p_j \psi_j(x,y) \text{ and } \mathbf{u} = \sum_{j=1}^{n} \mathbf{u}_j \phi_j(x,y),$$

is applied to equations (6). For consistency, we require $m \leq 2n$ as $n_f\beta_f \to 0$. This case resembles the classical Stokes' equations. For the classical Taylor-Hood elements, we use $\psi_i \in P_1(\Omega)$ and $\phi_i \in P_2(\Omega)$. Aguilar *et al.* [2] demonstrate for the one-dimensional Terzaghi problem by numerical experiments and the argument that the discretization matrix no longer remains an M-matrix if the time step satisfies $\Delta t < \frac{h}{6}$ that the numerical solution becomes mildly oscillatory. Aguilar *et al.* [2] use a stabilizator term of $\gamma\frac{\partial}{\partial t}\Delta p$ (with $\gamma = \frac{\sigma h^2}{4(\lambda+2\mu)} = O(h^2)$, where $\sigma = 1$) to suppress the spurious oscillations. In our application, the stabilization coefficient is given by $\gamma \approx 1.2 \cdot 10^{-18}$. We, however, think that the incompressible limit is mimiced by equation (7), and here the boundary conditions for the pressure in the problem of Aguilar *et al.* should be removed. Then, the equations can be tackled well with the LBB condition satisfying [8] Taylor-Hood elements.

In this study, we use linear-linear elements to solve equations (6). We verified numerically that these elements gave the same results as the Taylor-Hood elements. A possible reason for this is that for our settings the compressibility term is given by $n_f\beta_f \approx 2.5 \cdot 10^{-16}$, which is larger than the stabilization coefficient γ that was

introduced by Aguilar *et al.* [2]. Since this term, and in particular the $\frac{\partial p}{\partial \tau}$-term (also as $\Delta\tau \rightarrow 0$), gives an additional contribution to the diagonal entries of the discretization matrix, the M-matrix property of the discretization matrix is probably preserved. Hence, the right hand side of equation (7) stabilizes the solution. Note that linear-linear elements are always allowable if the stabilization term due to Aguilar is used. Our approach, which is motivated physically, stabilizes in a similar way as Aguilar's term does. We admit that this issue needs more investigation in mathematical rigor. For the concentrations and densities, linear elements are used too. The diffusion part of the equations for the mesenchymal cells and fibroblasts were solved using an IMEX method, where the diffusivities of the mesenchymal cells and fibroblasts were taken from the previous time step. The reaction parts in all the equations were treated using an IMEX time integration method too. The coupling was treated by the use of information from the previous time step. Until now, no iterative treatment of the coupling has been done in the current preliminary simulations. A state-of-the-art book on several numerical time integrators for stiff problems is the work due to Hundsdorfer & Verwer [10].

To determine the stimulus in equation (5), the strain is computed from the spatial derivatives of the displacements. To determine the strains at the mesh points, we proceed as follows: consider the equation for ε_{xx}, then multiplication by a test-function gives

$$\int_{\Omega} \varepsilon_{xx}\phi d\Omega = \int_{\Omega} \frac{\partial u}{\partial x}\phi d\Omega, \text{ for } \phi \in H^1(\Omega), \tag{8}$$

where $\varepsilon_{xx} \in H^1(\Omega)$. Using the set of basis functions as in our finite element solution, gives

$$\sum_{j=1}^{n} \varepsilon_{xx}^{j} \int_{\Omega} \phi_i \phi_j d\Omega = \sum_{j=1}^{n} u_j \int_{\Omega} \frac{\partial \phi}{\partial x}\phi_i d\Omega, \qquad \text{for } i \in \{1,\ldots,n\}. \tag{9}$$

This gives a system of n equations with n unknowns. This is applicable for any type of element. For piecewise linear basis functions, the mass matrix is diagonal (lumped) after applying Newton-Cotes' integration rule. Then, the strains and fluid velocities are used for the mechanical stimulus at the mesh points for the ordinary differential equations, which are solved using a time IMEX integrator only.

4 Numerical Experiments

In Figure 4 the distribution of the stimulus, osteoblast density, mesenchymal stem cell density and the bone fraction in the porous tantalum layer after 100 days have been plotted. The prosthesis is assumed to consist of two parts: the top part being the functional part on which an external force is exerted from the outer motion. The botton part is the porous tantalum, in which bone is allowed to grow in from the botton layer. The size of the prosthesis is given by 40×10 mm, in which the prosthesis is divided into the top and botton layer of the same size. The upper force

is given by 165.84 N, corresponding to an arm abduction of 30 degrees. In the top part of the prosthesis, the elasticity equations are solved. The prosthesis has been approximated by a two-dimensional geometry, which can be done with the use of cylindrical co-ordinates. The latter has not been done yet.

It can be seen that the osteoblast density is maximal where the stimulus is maximal. This implies that bone develops at the positions where the osteoblast density and stimulus is maximal. This can be seen clearly from the figures. Furthermore, the mesenchymal cell density shows a decrease where the cells differentiate into osteoblasts. The conditions are such that the model only allows the differentiation into osteoblasts and the development of other cell types and tissues is prohibited. To have bone ingrowth in the other parts of the tantalum, it is necessary that the upper arm moves allowing for the stimulus to increase at various positions within the tantalum. This has been observed to take place in preliminary simulations that are not shown in this paper. For arm abductions of 90 degrees, cartilage is also allowed to develop in the tantalum due to a higher outer force that is exerted on the top of the prosthesis. It can be seen that bone develops in the high stimulus domain. Bone remains can only remain at locations where it has been generated. Bone resorption has been disregarded in the model since its effect seems to be of second order only.

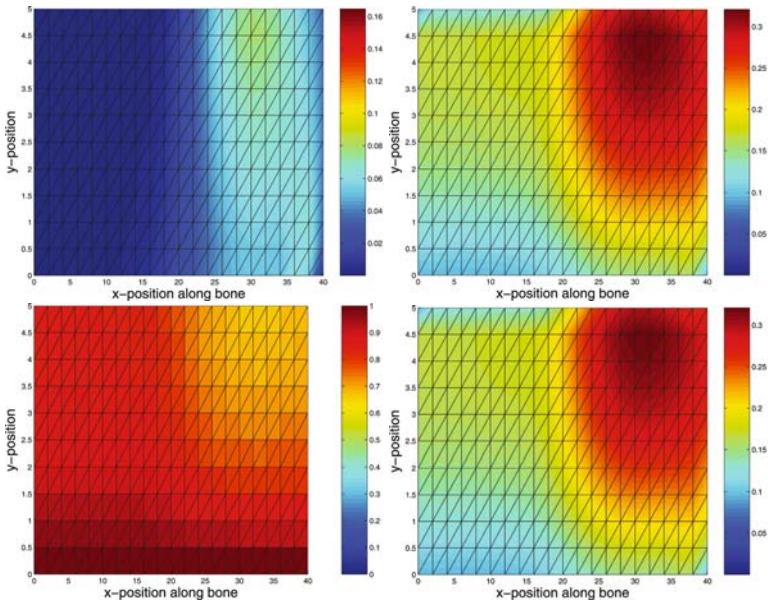

Fig. 2 Some distributions in the porous tantalum after 100 days: Left: The stimulus. Right: The osteoblasts (bone cells). Bottom-Left: The mesenchymal stemcells. Bottom-Right: The bone density.

Some preliminary results reveal that the model is rather insensitive to the diffusion parameters near the current values. There is a high sensitivity with respect to F_b, and Q_b in the present loading regime.

5 Conclusions

A model has been developed for bone-ingrowth into a prosthesis. Parameters that were used were obtained from literature and animal experiments. For small forces exerted, bone develops mainly near the interface and close to the applied force. For large forces, bone develops far away from the interface. For a complete ingrowth, oscillatory forces are to be applied. Linear-linear (displacement-pressure) elements are applicable for this two-dimensional problem.

References

1. Adam, J.: A simplified model of wound healing (with particular reference to the critical size defect). Mathematical and Computer Modelling **30**, 23–32 (1999)
2. Aguilar, G., Gaspar, F., Lisbona, F., Rodrigo, C.: Numerical stabilization of biot's consolidation model by a perturbation on the flow equation. International Journal of Numerical Methods in Engineering, submitted (2007)
3. Ament, C., Hofer, E.: A fuzzy logic model of fracture healing. Journal of Biomechanics **33**, 961–968 (2000)
4. Andreykiv, A.: Simulation of bone ingrowth. Thesis at the Delft University, Faculty of Mechanical Engineering (2006)
5. Bailon-Plaza, A., van der Meulen, M.C.H.: A mathematical framework to study the effect of growth factors that influence fracture healing. Journal of Theoretical Biology **212**, 191–209 (2001)
6. Bear, J.: Dynamics of fluids in porous media. American Elsevier Publishing Inc., New York (1972)
7. Braess, D.: Finite elements: theory, fast solvers, and applications in solid mechanics, 7 edn. Cambridge University Press, Cambridge (2007)
8. Gelhard, T., Lube, G., Olshanskiib, M., Starcke, J.: Stabilized finite element schemes with lbb-stable elements for incompressible flows. Journal of Computational and Applied Mathematics **177**, 243–267 (2005)
9. Huiskes, R., van Driel, W.D., Prendergast, P.J., Søballe, K.: A biomechanical regulatory model for periprosthetic fibrous-tissue differentiation. Journal of Materials Science: Materials in medicine **8**, 785–788 (1997)
10. Hundsdorfer, W., Verwer, J.G.: Numerical solution of time-dependent advection-diffusion-reaction equations. Springer Series in Computational Mathematics, Berlin-Heidelberg (2003)
11. LaCroix, D., Prendergast, P.: A mechano-regulation model for tissue differentiation during fracture healing: analysis of gap size and loading. Journal of Biomechanics **35 (9)**, 1163–1171 (2002)